Is a Large Bandwidth Mandatory to Maximally Exploit the Transmit Matched-Filter Structure?

Guido Carlo Ferrante, *Student Member, IEEE*

***Abstract*—Transmitted signals can be focused in time or space, i.e., at a particular receiver location, by introducing a prefilter in the transmitter. Prefiltering also allows containing intersymbol and multiuser interference. Performance bounds in terms of signal-to-noise ratio gain, which is achievable by prefiltering, depend on both transmitted signal bandwidth and channel characteristics. This paper analyzes the aforementioned dependence for transmit matched filters, which are also known as time-reversal prefilters, and channels with multipath. Theoretical results show that single-cluster channels verify a condition by which the gain is monotonic nondecreasing with bandwidth. Multicluster channels, such as those described by the Saleh–Valenzuela model, seem to follow a similar behavior, as suggested by simulation of the IEEE 802.15.3a channel model. As such, the transmit matched filter is particularly suitable for signals with large bandwidths, as in acoustics and ultrawideband communications.**

***Index Terms*—Transmit matched-filter, time-reversal, ultra-wideband (UWB), linear transceivers.**

I. Introduction

The interplay between transmitted signals, that are under designer's control, and channel, that is set by Nature, has an impact on system performance bounds. For systems with prefiltering, the dependence of performance bounds in terms of signal-to-noise ratio (SNR) on both bandwidth and channel has not been specifically addressed. For particular contexts, such as ultra-wideband (UWB) communications, the general claim is that the larger the bandwidth the higher the SNR. The intuition is that, while bandwidth grows, the prefilter can take advantage of an increased fraction of the channel; this intuition, however, has not been thoroughly investigated.

The goal of this paper is to address the above issue by investigating whether increased bandwidth implies increased SNR, when the channel is affected by multipath. To this end, two different transceiver structures are considered in the analysis. In the first structure, a simple pulse, i.e., a zero-excess bandwidth pulse as will be further defined, is transmitted. In the second structure, the same zero-excess bandwidth pulse is filtered by a transmit matched-filter [1]–[3], that has an impulse response proportional to the time-reversed version of the channel impulse response. In acoustics [4], [5], and UWB [6], this prefilter is known as time-reversal, although its first appearence may go back to [7], [8], where it was introduced as pre-Rake. These two structures are compared based on the SNR gain G, that is achievable by introducing prefiltering.

The paper is organized as follows: Section II contains the two reference system models and defines the system performance measure. Results are presented and discussed in Section III. Section IV contains the conclusion.

Manuscript received February 2, 2014; revised May 6, 2014 and May 29, 2014; accepted June 5, 2014. Date of publication June 10, 2014; date of current version September 8, 2014. The associate editor coordinating the review of this paper and approving it for publication was A. Ikhlef.

The author is with the Department of Information Engineering, Electronics and Telecommunications, Sapienza University of Rome, 00184 Rome, Italy, and also with the Département de Télécommunications, École Supérieure d'Électricité (Supélec), 91192 Gif-sur-Yvette, France.

Color versions of one or more of the figures in this paper are available online at http://ieeexplore.ieee.org.

Digital Object Identifier 10.1109/LCOMM.2014.2329849

II. System Model and Performance Measure

The two transceiver structures under analysis are shown in Fig. 1. No Intersymbol Interference (ISI) is assumed, e.g., either one symbol only, or symbol sequences with symbols modulating waveforms with vanishing crosscorrelations at the receiver, are transmitted.

In Structure 1, the transmitted signal is $x_1(t) = b\psi(t)$, where $\psi(t)$ has unit energy and b is the symbol to be transmitted, with $\mathbb{E}[|b|^2] = \mathcal{E}$. The noiseless received signal $y_1(t)$ is, as a function of frequency, $\hat{y}_1(f) = b\hat{\psi}(f)\hat{c}(f)$, where $\hat{c}(f)$ is the channel transfer function.

In Structure 2, the transmitted signal is $x_2(t)$. As a function of frequency, one has $\hat{x}_2(f) = \hat{x}_1(f) \cdot \sqrt{\xi}\hat{c}^*(f) = b\hat{\psi}(f)\sqrt{\xi}\hat{c}^*(f)$, where ξ is a constant such that $x_1(t)$ and $x_2(t)$ have same energy $\mathcal{E}$. Structure 2 requires a perfect knowledge of the channel at the transmitter. The noiseless received signal $y_2(t)$ is as a function of frequency: $\hat{y}_2(f) = \sqrt{\xi} \cdot b\hat{\psi}(f)|\hat{c}(f)|^2$.

In the two structures, $n(t)$ is a White Gaussian Noise process with spectrum height $\sigma^2 = \mathcal{N}_0/2$, and the receiver is a matched-filter followed by a sampler. Based on the no-ISI hypothesis, the channel can be modeled as Additive White Gaussian Noise (AWGN). In the first structure, the received signal $r_1(t) = y_1(t) + n(t)$ is projected onto a waveform proportional to $y_1(t)$. In the second structure, $r_2(t) = y_2(t) + n(t)$ is projected onto a waveform proportional to $y_2(t)$. The projection of the generic received signal $r_k(t)$ onto $y_k(t)$, $k \in \{1, 2\}$, is:

$$\begin{aligned}\langle r_k, y_k\rangle = \langle \hat{r}_k, \hat{y}_k\rangle &\triangleq \int_{\mathbb{R}} \hat{r}_k(f)\hat{y}_k^*(f)df \\ &= \langle \hat{y}_k, \hat{y}_k\rangle + \nu_k,\end{aligned} \tag{1}$$

where ν_k is a real Gaussian random variable (r.v.) with $\mathrm{Var}[\nu_k] = \sigma^2\langle \hat{y}_k, \hat{y}_k\rangle = \sigma^2\|\hat{y}_k\|^2$. The SNR at the receiver, after the sampler, is:

$$\mathsf{SNR}_i \triangleq \frac{\mathbb{E}\left[|\langle \hat{y}_i, \hat{y}_i\rangle|^2\right]}{\mathrm{Var}[\nu_i]}. \tag{2}$$

With reference to Fig. 1, one has $\mathsf{SNR}_1 = (\mathcal{E}/\sigma^2) \cdot \|\hat{\psi}\hat{c}\|^2$ and $\mathsf{SNR}_2 = (\mathcal{E}/\sigma^2) \cdot \|\hat{\psi}|\hat{c}|^2\|^2/\|\hat{\psi}\hat{c}\|^2$.

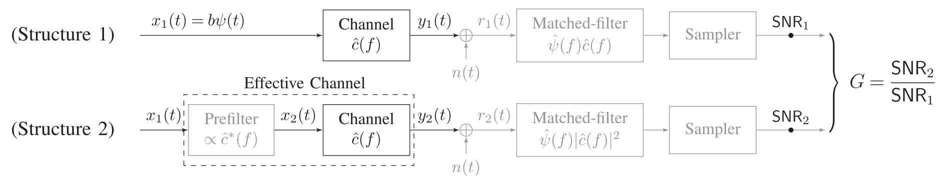

Fig. 1. The two reference system models. Structure 1 corresponds to a traditional transmission with no prefiltering at the transmitter and matched-filtering at the receiver. Structure 2 corresponds to prefiltering at the transmitter with transmit matched-filter, and matched-filtering at the receiver. In both structures, $\psi(t)$ is a zero-excess bandwidth waveform. It is assumed that prefiltering does not alter energy, that is, $x_1(t)$ and $x_2(t)$ have same energy $\mathcal{E}$.

Gain G allows comparison of the two structures and is defined as follows:

$$G \triangleq \frac{\mathsf{SNR}_2}{\mathsf{SNR}_1} = \frac{\left\|\hat{\psi}|\hat{c}|^2\right\|^2}{\|\hat{\psi}\hat{c}\|^4}. \tag{3}$$

For the sake of simplicity, $\psi(t)$ is assumed as a zero-excess bandwidth waveform with band $[-W/2, W/2]$, i.e., $\psi(t) = \sqrt{W}\operatorname{sinc}(\pi W t)$, where $\operatorname{sinc} x \triangleq (\sin x)/x$, for which SNR_1 and SNR_2 become:

$$\mathsf{SNR}_1 = \frac{\mathcal{E}}{\sigma^2} \cdot \frac{1}{W} \int_{-\frac{W}{2}}^{\frac{W}{2}} |\hat{c}(f)|^2 \, df, \tag{4}$$

$$\mathsf{SNR}_2 = \frac{\mathcal{E}}{\sigma^2} \cdot \int_{-\frac{W}{2}}^{\frac{W}{2}} |\hat{c}(f)|^4 \, df \bigg/ \int_{-\frac{W}{2}}^{\frac{W}{2}} |\hat{c}(f)|^2 \, df, \tag{5}$$

and gain G is:

$$G = W \cdot \frac{\int_{-\frac{W}{2}}^{\frac{W}{2}} |\hat{c}(f)|^4 \, df}{\left[\int_{-\frac{W}{2}}^{\frac{W}{2}} |\hat{c}(f)|^2 \, df\right]^2} = \frac{W}{2} \cdot \frac{\int_0^{\frac{W}{2}} |\hat{c}(f)|^4 \, df}{\left[\int_0^{\frac{W}{2}} |\hat{c}(f)|^2 \, df\right]^2}. \tag{6}$$

Gain G also provides a hint on performance in the coded regime, as measured by maximal mutual information $I_k = 1/2 \ln(1 + \mathsf{SNR}_k)$, $k \in \{1, 2\}$, nats/channel use. Since the system is baseband, the no-ISI hypothesis holds, for example, by making the symbol period T_s greater than the channel delay spread T_d, by which $I_k = (1/T_s) \cdot (1/2) \ln(1 + \mathsf{SNR}_k)$ nats/s. Similarly to the SNR gain G, an *information gain* G_I can be defined as follows:

$$G_I \triangleq \frac{I_2}{I_1} = \frac{\ln(1 + \mathsf{SNR}_2)}{\ln(1 + \mathsf{SNR}_1)} = \frac{\ln(1 + G \cdot \mathsf{SNR}_1)}{\ln(1 + \mathsf{SNR}_1)}.$$

In the low-SNR regime ($\mathsf{SNR}_k \ll 1$, $k \in \{1, 2\}$) one has $G_I \approx \mathsf{SNR}_2/\mathsf{SNR}_1 = G$, hence G_I reduces to G. In the high-SNR regime ($\mathsf{SNR}_k \gg 1$) one has $G_I \approx \ln(\mathsf{SNR}_2)/\ln(\mathsf{SNR}_1) = 1 + \ln(G)/\ln(\mathsf{SNR}_1)$, and for channels with bounded G, e.g., multipath channels, G_I reduces to unity as $\mathsf{SNR}_1 \to \infty$. G is, therefore, the most important parameter to be analyzed to determine performance of systems in both uncoded and coded regimes, under the no-ISI hypothesis.

III. System Analysis Based on Gain G

In this section, we find the lower bound of G and the asymptotic value of G as $W \to \infty$ for multipath channels (Section III-A), and derive a necessary and sufficient condition for G to be a monotonic non-decreasing function of W, also showing examples and counterexamples of channels verifying the condition (Section III-B).

A. Gain G Limit Values

1) Lower Bound of G: By applying the Cauchy-Schwarz inequality to the denominator of eq. (3), one has $\|\hat{\psi}\hat{c}\|^2 = \langle \hat{\psi}, \hat{\psi}\hat{c}^*\hat{c} \rangle \leq \|\hat{\psi}\| \cdot \|\hat{\psi}\hat{c}^*\hat{c}\|$. Therefore, $G \geq 1$, implying that Structure 2 in Fig. 1 cannot underperform Structure 1. Equality is achieved iff $\hat{\psi} \propto \hat{\psi}\hat{c}^*\hat{c}$, i.e., iff $|\hat{c}(f)|$ is constant for $f \in \operatorname{supp} \hat{\psi} \triangleq \{\nu \in \mathbb{R} : \hat{\psi}(\nu) \neq 0\}$, as can also be directly shown by methods of variational calculus. The minimum gain $G = 1$ is thus obtained when the magnitude of the channel transfer function is nonzero and flat, for frequency intervals where the amplitude of the spectrum of transmitted signals is nonzero. Typically, this is true when the channel is perfect (channel transfer function with constant amplitude) at least within the transmitted signal bandwidth. This condition easily holds for narrowband communications.

2) Asymptotic Value of G as $W \to \infty$: Consider the following multipath channel:

$$c(t) = \sum_{k \geq 0} \alpha(\tau_k) \delta(t - \tau_k), \tag{7}$$

where τ_k and $\alpha(\tau_k) \in \mathbb{R}$ are delay and amplitude of ray k. Eq. (7) also models realizations of channels with clusters. Supposing that a same interarrival time between two consecutive rays is not possible,[1] it can be shown that [9], as $W \to \infty$, the gain is:

$$G = 2 - \sum_{k \geq 0} \alpha(\tau_k)^4 \bigg/ \Big[\sum_{k \geq 0} \alpha(\tau_k)^2\Big]^2, \tag{8}$$

and, therefore, $G < 2$ irrespective of channel amplitudes.

B. Slope of G vs. W

From above, G is bounded as follows:

$$1 = \lim_{W \to 0} G(W) \leq \lim_{W \to \infty} G(W) < 2.$$

In this section, the condition by which $G(W)$ is a monotonic non-decreasing function is derived. For the sake of generality, the condition is derived for random channels, but it can be applied

[1]This hypothesis often holds with probability one for random channels, since interarrival times are usually independent.

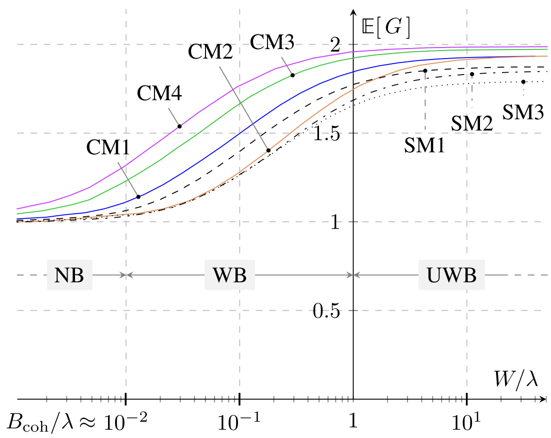

Fig. 2. Average gain $\mathbb{E}[G]$ vs. W/λ for channel models CM1-CM4 of the IEEE 802.15.3a standard [10], and single-cluster models SM1-SM3, that refers to channel of eq. (7), with parameters $(\lambda, \gamma, \sigma_{\rm r})$ equal to (2, 4, (1/2)), (2, 2, (1/4)) and (2, 2, (1/2)), respectively, where $1/\lambda$ and γ are expressed in nanoseconds.

to nonrandom channels as well. Suppose that $G(W)$ is random, with average $\mathbb{E}[G]$. The slope of $\mathbb{E}[G]$ is nonnegative iff:

$$\frac{d}{dw}\mathbb{E}[G] \geq 0, \qquad \forall w > 0, \tag{9}$$

where $w \triangleq W/2$.

Fig. 2 shows $\mathbb{E}[G]$ vs. W/λ obtained by means of Monte-Carlo simulations for UWB channels following the IEEE 802.15.3a standard model [10], where $1/\lambda$ is the average intra-cluster interarrival time between two rays, with values in the range [0.4,2] nanoseconds. Fig. 2 suggests that channel models valid for very large bandwidths, up to several gigahertz, verify eq. (9).

Also shown in Fig. 2 is when a signal can be considered as narrowband, wideband or UWB, as a function of the statistical parameters of the channel it experiences. In a multipath channel, most of the power lies in $[0, T_d]$, i.e., $[0, 1/B_{\rm coh}]$, where $B_{\rm coh}$ is the *coherence bandwidth*. When $W < B_{\rm coh}$, there is about only one resolved path. $B_{\rm coh}$ may serve, therefore, to define narrowband signals, the condition being $W < B_{\rm coh}$. Similarly, λ may define UWB signals, the condition being $W > \lambda$, for which a significant fraction of the multipath components can be resolved. For $W \in [B_{\rm coh}, \lambda]$, the signal may be considered as wideband.

In general, a direct computation of $\mathbb{E}[G]$ is a formidable task, even for simple models that do not account for clustering. Therefore, a condition, that does not require the explicit knowledge of $\mathbb{E}[G]$, for eq. (9) to hold, is derived below.

Proposition 1: Let $\hat{c}(f)$ be the frequency response of a realization of a random multipath channel, and denote by $S(f) = |\hat{c}(f)|^2$ its squared magnitude. Then $\mathbb{E}[G]$ is a monotonic nondecreasing function, i.e., condition of eq. (9) holds, iff:

$$\begin{aligned} F(w) \triangleq\; & \frac{1}{w^2}\int\!\!\int_{[0,w]^2} \mathbb{E}\left[S(f_1)S(f_2)^2\right] df_1 df_2 \\ & + \frac{1}{w}\int_{[0,w]} \mathbb{E}\left[S(f)S(w)^2 - 2S(f)^2 S(w)\right] df \geq 0. \end{aligned} \tag{10}$$

Proof: Interchange differentiation and expectation operators in eq. (9), and compute dG/dw; then discard the denominator, since it is always positive, and interchange the order of expectations and integrations. □

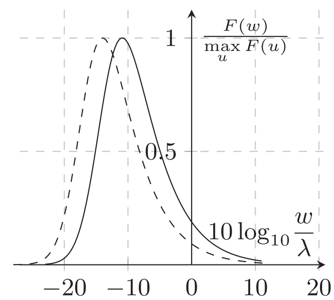

Fig. 3. $(F(w)/\max_u)F(u)$ vs. w/λ (dB) for the single-cluster channel model and different $(\lambda, \gamma, \sigma_{\rm r})$ configurations. Solid curve: (2, 2, (1/2)), (2, 2, (1/4)). Dashed curve: (4, 2, (1/2)), (2, 4, (1/2)). $1/\lambda$ and γ are expressed in nanoseconds. $F(w)$ is positive, showing that eq. (10) is verified.

Note on eq. (10) that $F(w)$ is the derivative of $\mathbb{E}[G]$ up to a positive factor depending on $|\hat{c}(f)|^2$.

An example of a channel model that verifies eq. (10) is the "Single-cluster Model" (SM). This model is similar to the IEEE 802.15.3a-CM1 [10] when restricted to the first cluster. In particular, the SM channel impulse response is given by eq. (7), where $\{\tau_k\}_{k\geq 0}$ and $\{\alpha(\tau_k)\}_{k\geq 0}$ are random variables. Interarrival times $\{\tau_{k+1} - \tau_k\}_{k\geq 0}$ are independent and exponentially distributed with average $\mathbb{E}[\tau_{k+1} - \tau_k] = 1/\lambda$. Conditioned on τ_k, the distribution of the path amplitude $\alpha(\tau_k)$ is an even function, and $|\alpha(\tau_k)|$ follows a log-normal distribution. Even conditional moments are $\mathbb{E}[\alpha(\tau)^{2n}|\tau] = (\Omega_0 e^{-(\tau/\gamma)})^n e^{2n(n-1)\sigma_{\rm r}^2}$ for $n \geq 1$, where $\gamma > 0$ is the ray decay factor, $\sigma_{\rm r}$ is the standard deviation of the Gaussian r.v. generating the log-normal r.v., and Ω_0 is the variance of $\alpha(0)$. Odd conditional moments are nil. In order to compute $\mathbb{E}[S(f_1)S(f_2)^2]$, the approach proposed in [11] for $\mathbb{E}[S(f_1)S(f_2)]$ is generalized here:

$$\begin{aligned} &\mathbb{E}\left[\prod_{i=1}^{M} S(f_i)\right] \\ &= \mathbb{E}\left\{\sum_{k_1\geq 0}\cdots\sum_{k_{2M}\geq 0} \mathbb{E}\left[\prod_{m=1}^{2M}\alpha(\tau_{k_m})|\,\{\tau_{k_n}\}_{n=1}^{2M}\right]\right. \\ &\qquad\left. \exp\left[-j2\pi\sum_{\ell=1}^{M} f_\ell(\tau_{k_{2\ell-1}} - \tau_{k_{2\ell}})\right]\right\}, \end{aligned} \tag{11}$$

that, for $M = 3$ and $f_3 \to f_2$, provides $\mathbb{E}[S(f_1)S(f_2)^2]$. In the right-hand side of eq. (11), the inner expectation is over amplitudes conditioned on delays $\{\tau_{k_m}\}_{m=1}^{2M}$, and the outer expectation is over delays only. Inner expectations are nonzero iff the set $\{\alpha(\tau_{k_1}), \ldots, \alpha(\tau_{k_{2M}})\}$ can be partitioned into subsets with even cardinality. With probability one, the set of indices $\{k_1, \ldots, k_{2M}\}$ can be equivalently partitioned. Logical conditions ensuring the partition can be derived. In the simple case of $M = 2$, there are four logical conditions, i.e., $k_1 = k_2 = k_3 = k_4$; $k_1 = k_2 \neq k_3 = k_4$; $k_1 = k_3 \neq k_2 = k_4$; $k_1 = k_4 \neq k_2 = k_3$. For $M = 3$, there are 31 logical conditions, that are not reported here for brevity. Once the conditions are set, the closed form expression of $\mathbb{E}[S(f_1)S(f_2)^2]$ can be derived, since each inner expectation is equal to an even conditional moment with appropriate order. Fig. 3 represents $F(w)$, normalized to

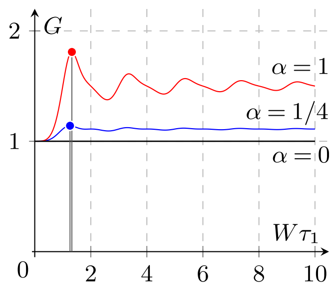

Fig. 4. Gain G vs. $W\tau_1$ for the two-paths channel $c(t) = \delta(t) + \alpha\delta(t - \tau_1)$ with $\alpha \in \{0, (1/4), 1\}$. For $\alpha \neq 0$, G is not monotonic non-decreasing: there exist local maxima and minima, and a global maximum (see dots) with respect to $W\tau_1$ (indicated by vertical lines) depending on α.

its maximum, for different γ and σ_r values, and shows that $F(w)$ is positive for any relevant w.

A channel that does not verify eq. (10) is as simple as a two-paths nonrandom channel with impulse response $c(t) = \delta(t) + \alpha\delta(t - \tau_1)$, $\alpha \in \mathbb{R}$, $\tau_1 > 0$. Since the channel is nonrandom, $\mathbb{E}[G] = G$. The channel frequency response squared magnitude is:

$$S(f) = |\hat{c}(f)|^2 = 1 + \alpha^2 + 2\alpha\cos(2\pi f\tau_1). \qquad (12)$$

The limit case $\alpha = 0$ reduces to the channel with constant spectrum (c.f. Section III-A). The value of G as $W\tau_1 \to \infty$ is $(1 + 2\alpha^2)/(1 + \alpha^2)^2$, that is maximum for $|\alpha| = 1$, for which $G = 3/2$. Fig. 4 shows G vs. $W\tau_1$ for $\alpha \in \{0, (1/4), 1\}$. Note that, for any fixed α, there exists an optimum $W\tau_1$ that maximizes G (see dots on figure for $\alpha = 1/4$ and $\alpha = 1$). For example, for $\alpha = 1$, the maximum gain is reached for $W\tau_1 \approx 1.32465$, and is equal to $G \approx 1.80905$. Fig. 4 shows that G is not monotonic non-decreasing with W for any α.

IV. Conclusion

This paper investigated whether a large bandwidth is mandatory to maximally exploit the potential benefits of the transmit matched-filter, in the absence of ISI. To this end, two transceiver structures, with and without prefiltering, were compared based on a parameter indicating the SNR gain G achieved by introducing the prefilter. Performance depended on both transmitted signal bandwidth W and channel frequency response squared magnitude. Limit values of G when the channel is affected by multipath were derived, for $W \to 0$ and $W \to \infty$, and it was proven that G for $W \to 0$ reaches the minimum, and is equal to one. A condition for G to be a monotonic non-decreasing function of W was also derived for generic random channels. This condition was then specified for single-cluster multipath channel models, and verified in the particular case of exponentially distributed interarrival times and absolute path amplitudes following a log-normal distribution. Simulation experiments of channels following the IEEE 802.15.3a standard channel model showed a monotonic non-decreasing gain in W for the four models of the standard, suggesting that G may also be monotonic non-decreasing for channels with clusters. However, the analysis of a channel with two paths only was shown to be a very simple counterexample, for which the gain was not a monotonic function of W.

In conclusion, a large bandwidth is not mandatory to achieve a maximum gain with transmit matched filter, although this seems to be the case for models describing realistic channels, such as the IEEE 802.15.3a model.

Results were obtained in terms of SNR gain G. As discussed in Section II, an information gain G_I can be defined, similarly to G, as the ratio between the mutual information achieved with and without prefiltering. It was proven that, under the no-ISI hypothesis, G_I essentially reduces to G. This would be no longer true if the no-ISI hypothesis were removed, in which case an achievable "capacity gain" should be analyzed. This will be the goal of future work together with two generalization: 1) channel models that expand beyond multipath; 2) prefilter structures that expand beyond transmit matched-filters. Preliminary investigations focusing on Gaussian vs. bandpass channels suggest that, in this case, G may be unbounded due to dramatic loss of efficiency without prefiltering.

Finally note that a prefilter that is proportional to $(\hat{c}^*(f)/(|\hat{c}(f)|^2 + \lambda))$ encompasses transmit zero-forcing and transmit MMSE, for particular values of λ, and therefore the current setting may serve towards a deeper understanding of prefiltering effects beyond the transmit matched-filter case.

References

[1] M. Joham, W. Utschick, and J. Nossek, "On the equivalence of prerake and transmit matched filter," in *Proc. 10th Aachen Symp. Signal Theory*, Aachen, Germany, 2001, pp. 313–318.

[2] M. Joham, W. Utschick, and J. Nossek, "Linear transmit processing in MIMO communications systems," *IEEE Trans. Signal Process.*, vol. 53, no. 8, pp. 2700–2712, Aug. 2005.

[3] M. Joham, K. Kusume, M. H. Gzara, W. Utschick, and J. A. Nossek, "Transmit Wiener filter for the downlink of TDD DS-CDMA systems," in *Proc. IEEE 7th ISSSTA*, Prague, Czech Republic, 2002, pp. 9–13.

[4] A. Derode, P. Roux, and M. Fink, "Robust acoustic time reversal with high-order multiple scattering," *Phys. Rev. Lett.*, vol. 75, no. 23, pp. 4206–4209, Dec. 1995.

[5] M. Fink, G. Montaldo, and M. Tanter, "Time reversal acoustics," in *Proc. IEEE Ultrason. Symp.*, Montreal, QC, Canada, 2004, vol. 2, pp. 850–859.

[6] T. Strohmer, M. Emami, J. Hansen, G. Papanicolaou, and A. Paulraj, "Application of time-reversal with MMSE equalizer to UWB communications," in *Proc. IEEE GLOBECOM*, Dallas, TX, USA, 2004, vol. 5, pp. 3123–3127.

[7] R. Esmailzadeh and M. Nakagawa, "Pre-rake diversity combination for direct sequence spread spectrum communications systems," in *Proc. IEEE ICC*, Geneva, Switzerland, 1993, vol. 1, pp. 463–467.

[8] R. Esmailzadeh and M. Nakagawa, "Pre-rake diversity combination for direct sequence spread spectrum mobile communications systems," *IEICE Trans. Commun.*, vol. 76, no. 8, pp. 1008–1015, Aug. 1993.

[9] G. C. Ferrante, "Time-reversal against optimum precoder over frequency-selective channels," in *Proc. 18th European Wireless Conf.*, Poznan, Poland, 2012, pp. 1–8.

[10] J. Foerster, "Channel modeling sub-committee report final," IEEE, Piscataway, NJ, USA, Tech. Rep. Doc. P802.15-02/490r1-SG3a, 2003.

[11] W.-D. Wu, C.-C. Lee, C.-H. Wang, and C.-C. Chao, "Signal-to-interference-plus-noise ratio analysis for direct-sequence ultra-wideband systems in generalized Saleh-Valenzuela channels," *IEEE J. Sel. Topics Signal Process.*, vol. 1, no. 3, pp. 483–497, Aug. 2007.